

A High Dynamic Range CMOS APS Image Sensor

By: Yibing (Michelle) Wang, Sandor L. Barna*, Scott Campbell and Eric R. Fossum
Photobit Technology Corp., *Photobit Corp.
135 N. Los Robles Ave, 7th floor, Pasadena, CA 91101
mwang@photobit.com

Abstract

In this paper, a new visible image sensor with 110 dB intrascene dynamic range is reported. The sensor captures four linear response images with different sensitivities simultaneously at 60 frames per second (fps). A real time fusion and dynamic range compression (DRC) algorithm, which is implemented by an FPGA, is also presented. This algorithm can generate a high dynamic range image from the four images of different sensitivity, compresses the composite image's dynamic range to match that of a normal 8-bit display unit, and displays it at video rate (60 fps). Finally, an accurate measurement method in determining the sensor's dynamic range is also presented.

I. Introduction

Real scenes produce a wide range of brightness variations, while the dynamic range of the typical solid-state image sensor is much lower - about 60 to 70 dB for CCDs and CMOS Active Pixel Sensors (APS). This results in low quality images where details in the scene are concealed in shadows or washed out by bright lights.

In this research, a new visible high dynamic (HiDy) range image sensor with 108 dB intrascene dynamic range is proposed, designed and tested. We introduce a new sensor architecture that can capture four linear response images with different sensitivities simultaneously. This technique eliminates the need for devices with logarithmic response, which reduce the image contrast, and avoids taking several sequential images at different exposures, which introduces motion blur to the final image. This research also proposes a real time fusion and dynamic range compression algorithm which generates a high dynamic range image from the four images of different sensitivity, compresses the composite image's dynamic range to match that of a normal 8-bit display unit, and displays it at video rate.

II. Architecture of HiDy Sensor

A photogate APS pixel with anti-blooming/shuttering capability, which was

developed by Fossum *et al.* [1], and reported by Yang *et al.*[2] and Barna *et al.* [3], is chosen for the new high dynamic range sensor. The photogate pixel, which is shown in Figure 1, inherently has two photoelectron collection regions, one is the photogate (PG) region, the other is the floating diffusion (FD). Typically the FD region is much smaller than the PG region, and often is covered by a dark layer (e.g. metal). However, the FD can still laterally collect charge generated in other regions of the pixel, and it is much less sensitive than the PG region. Thus, the PG signal can be used for image capturing under low light and the FD signal, which is also called the shuttered photodiode (SPD) signal, can be used under bright light without changing the iris setting of the camera. This dual-sensitivity characteristic was first explored by Barna *et al.* in [3].

In this research, the dual-sensitivity feature of the photogate pixel is explored further for intrascene dynamic range extension. We capture two images of different sensitivities, PG and SPD image, simultaneously by using one photogate pixel array. The two original images from the photogate array are multiplied by two different gains to form four images of different sensitivities. Figure 2 shows the analog processing scheme of the HiDy sensor. These four images can be combined together to generate a high dynamic range image with more than 100 dB intrascene dynamic range. The advantages include higher frame rate, less distortion when the object is moving and no requirement for external frame memory.

At this time, a HiDy sensor chip has been designed and tested. There is no control logic or image post-processing unit on chip. Four on-chip ADCs are used to digitize the four analog image outputs into four 8-bit digital outputs. This chip is fabricated using a standard two-poly-three-metal (2P3M) CMOS process. The chip can operate at 60 frames per second. It has a dynamic range of 108 dB or 18 bits. Because 8-bit flash ADCs are used to digitize the original images, the signal-to-noise ratio (SNR) is approximately 48 dB for each of the digital outputs. The pixel array size is 352×288 , which is the common

intermediate format (CIF). The die size is 8.8 mm × 10.5 mm. The total power dissipation is 750 mW, which is due, in large part, to the four flash-type ADCs on the chip.

III. Image Fusion and Dynamic Range Compression (DRC)

This section will discuss the fusion algorithm used to combine the four images taken by the high dynamic range image sensor, and the method used to compress the dynamic range of the fused high dynamic range image for display using normal 8-bit display devices.

Before going into details of the fusion and DRC algorithm we developed, the human vision system will first be briefly reviewed. Our intention is to choose an algorithm which is not only simple for hardware implementation, but also has a response similar to that of the human eye.

The range of light intensity levels to which the human visual system can adapt is about 200 dB. The experimental result shows that subjective brightness is a logarithmic function of the light intensity incident on the eye. However, the visual system can by no means operate over such a range simultaneously. Rather, it accomplishes this large variation by changes in its overall sensitivity, a phenomenon known as brightness adaptation. The total range of intensity levels it can discriminate simultaneously is rather small when compared with the total adaptation range. For any given set of conditions, the current sensitivity level of the visual system is called the brightness-adaptation level. Normally, the scene to see is much bigger than the area that the eye can see simultaneously. As the eye roams about the scene, the eye's focus is changed from point to point, and the instantaneous adaptation level fluctuates about the average level that depends on the properties of the focus point [4].

Based on the above brief review, to match HVS's response, the fusion and DRC algorithm should take into account the overall subjective brightness response as well as the brightness adaptation effect. Only by doing these can we get a final image for display that best match the subjective viewing experience our eyes get when looking at the same scene.

For the high dynamic range sensor we developed, we use a nonlinear fusion algorithm which aggregates the images of different sensitivities to create the fused image. It is very simple for hardware implementation. No brightness information is lost, and by selecting

suitable aspect ratios between different images to cover the whole operating range, the output to illuminance response curve can be very close to the logarithmic compression curve characteristic of the human visual system [4]. This compression of the output means the output pin requirement of the sensor is greatly reduced. For example, if there are four 8-bit images of different sensitivities simultaneously output from the sensor, four 8-bit wide data busses are needed. If the linearly fused image is output, the data bus must be 20 bits wide for a dynamic range of 120 dB. The sum of the four images is only a 10-bit image, which requires only one 10-bit data bus.

Since the normal display devices can only take 8-bit input, dynamic range compression is still necessary to compress the 10-bit fused image into 8-bit image. An adaptive histogram modification algorithm was developed for this purpose. It closes the gaps of the sparsely populated luminance values, or in other words, closes the gaps of different adaptation levels.

The basic idea of adaptive histogram modification algorithm is to compress the dip areas of the histogram, which associate with the gaps between different adaptation levels, only. We first set a threshold number H_{th} , which is used to identify the dip areas, and define $F(g)$ as the compressed gray level output. Then start to scan the histogram of the given image from left to right (small gray values to large gray values). If the histogram value $H(g)$ of the current gray level g is smaller than H_{th} , then this gray level g is in the dip. And it will share the same gray level output as its previous gray level $g - 1$, which is $F(g) = F(g - 1)$. If the histogram value $H(g)$ is larger than H_{th} , then do not compress and the output is $F(g) = F(g - 1) + 1$.

If we follow the above simple procedure, many times if the dip areas are large, which means that there is a large number of pixels falling into these areas, the resulting histogram will generate some new peaks, which introduce visible noise to the final image. To prevent from generating unwanted peaks, we set another threshold number N_{th} to limit the total number of pixels which share the same output gray level and break a large dip area into smaller areas. We compare the value of a running sum function $S(H(gc), H(gc + 1), \dots, H(g))$ with the threshold N_{th} (here gc is the starting gray level of the dip area, and g is the current gray level). When it reaches N_{th} , the current gray level g will be set as a new starting gray level gc . As a result,

one large area is broke into some smaller areas and compressed separately.

The fusion and DRC algorithms have been implemented on a Xilinx FPGA. It takes about only 50,000 gates and 18 Kbit memory to implement it. Thus, it will be very compact to integrate such a processor on-chip together with the sensor array. The inputs of the FPGA are the four 8-bit image outputs from the HiDy sensor chip, and the output of the FPGA is the final 8-bit image ready for display. The output video rate of the FPGA is also 60 fps. Figure 3 shows four original image outputs from the HiDy sensor, and Figure 4 shows the final image output from the FPGA. The dynamic range of this scene is about 95 dB.

IV. Dynamic Range Measurement

To implement an accurate measurement method in determining the sensor's dynamic range, we considered the use of Fraunhofer diffraction from a circular aperture. This is an effect of great practical significance in the study of optical instrumentation [5]. The Fraunhofer diffraction pattern from an aperture (also called the aperture's "far-field" pattern) is very similar in nature to the Fourier transform of that aperture. Due to its deterministic nature, a known aperture's Fraunhofer diffraction pattern can be very useful in the lensless yet structured illumination of image sensors. For example, if a monochromatic, planewave light beam passes through a circular aperture, then the far field pattern observed is a number of concentric rings, about a central lobe, with increasing radius but decreasing intensity. In this case, the particular far field pattern is called the Airy disk pattern. The irradiance of this pattern follows the

function $I(u) \left[\frac{2J_1(u)}{u} \right]^2$, where $I(0)$ is the peak

intensity at the center of the pattern, $J_1(u)$ is the first order Bessel function, and u is a function of the wavelength of the light used, the radius of the aperture's opening, the distance between the far field plane and the aperture, and the radial distance between the point calculated and the central point of the pattern. The normalized irradiance map along the radius from the center to a given field point is shown in Figure 5. A detailed explanation of this effect can be found in [5]. By capturing an image of the Airy disk pattern (without saturating its central lobe) and then counting the number of rings detected, it is

therefore straightforward to appropriately determine the dynamic range of the sensor.

The test setup to accomplish the above-discussed measurement of the sensor's dynamic range involves placing a pinhole (the aperture) some (far field) distance in front of a sensor array (with no a lens present). The light source used to irradiate the pinhole is then a planewave laser beam, directed to pass through the pinhole orthogonal to both the pinhole and the sensor such that the sensor will capture the diffraction pattern from the pinhole. Figure 6 displays such a diffraction pattern captured by a Hidy sensor when using a 50 μm pinhole and a 633 nm wavelength laser beam. Figure 7 shows the final image which is fused and dynamic range compressed from the four original images in Figure 6. There are approximately 30 rings detectable in the individual images and the final image. Thus, by examining Figure 5, the sensor's full dynamic range can be determined to be approximately 110 dB.

V. Conclusions:

In this paper, a new linear response CMOS APS sensor with 110 dB dynamic range is presented. The image fusion and dynamic range compression algorithms we proposed match the subjective viewing experience of human visual system, and are simple and easy for on-chip integration.

References

- [1] E.R. Fossum, *et al.*, "Active pixel sensor array with electronic shuttering", *U.S. Patent Application CIT Case #2247-2B*, Jet Propulsion Laboratory, California Institute of Technology.
- [2] G. Yang, *et al.*, "A snap-shot CMOS active pixel imager for low-noise, high-speed imaging", *IEEE International Electron Devices Meeting, 1998 Technical Digest*, Session 2, Paper 7, 1998.
- [3] S.L. Barna, *et al.*, "A low-light to sunlight, 60 frames/s, 80 kpixel CMOS APS camera-on-a-chip with 8b digital output", *Proc. of the 1999 IEEE Workshop on Charge-Coupled Devices and Advanced Image Sensors*, Karuizawa, Japan, June 1999.
- [4] R.C. Gonzalez and R.E. Woods, *Digital Image Processing*, Addison-Wesley, Sept. 1993.
- [5] E. Hecht, *Optics*, Addison-Wesley, 1974.

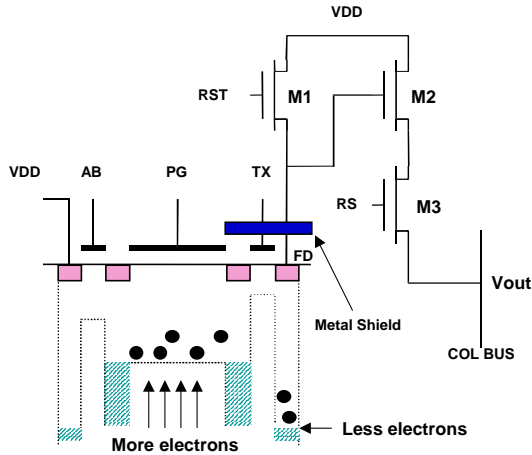


Figure 1 The architecture of photogate pixel with antiblooming control.

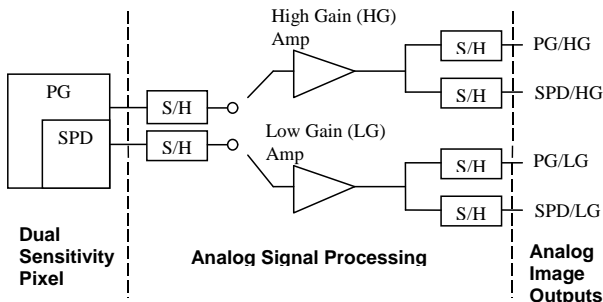


Figure 2 The description of analog processing scheme of HiDy sensor. The outputs from each dual-sensitivity pixel are sampled-and-held first, then go through the high gain and low gain amplifiers to become four analog outputs.

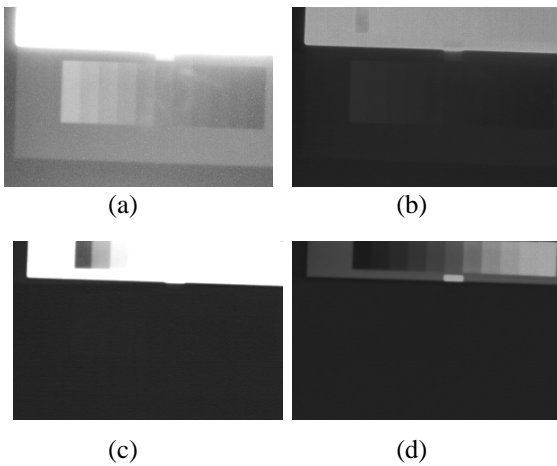


Figure 3 HiDy sensor outputs. (a) PG high gain. (b) PG low gain. (c) SPD high gain. (d) SPD low gain.

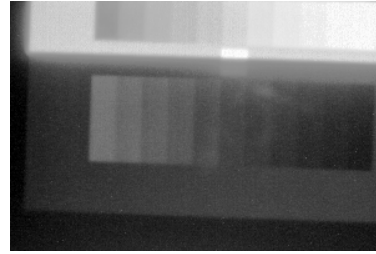


Figure 4 Fused and dynamic range compressed image from the four original images in Figure 3.

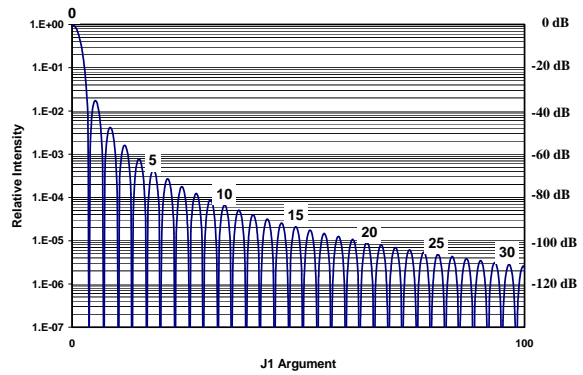


Figure 5 Intensity distribution in the diffraction pattern of a circular aperture.

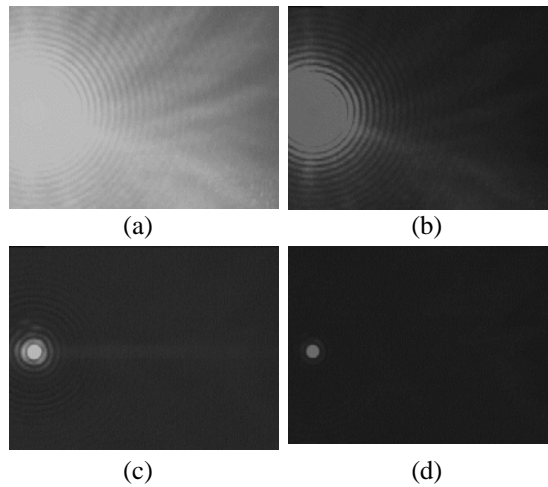


Figure 6 Diffraction pattern of a 50µm pinhole captured by HiDy sensor.

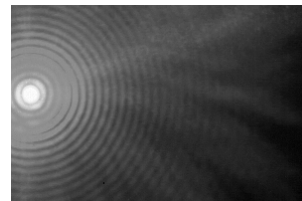


Figure 7 Final image of the diffraction pattern of Figure 6.